

no reports on total porphyrin analysis including analysis of porphyrin isomers. In this study, it was attempted to verify the results obtained by Ogura et al. in humans by improving pretreatment for porphyrins in plasma and mobile-phase gradient conditions for HPLC with the use of a reversed-phase column in order to separate and quantify total porphyrins including porphyrin isomers in an accurate manner.

Materials and Method

1. Reagents

The following materials were purchased from Frontier Scientific, Inc.: porphyrin acid chromatographic marker kit (hereinafter abbreviated to "Kit" containing uroporphyrin I (hereinafter abbreviated to "UPI"), heptaporphyrin (hereinafter abbreviated to "7P"), hexaporphyrin (hereinafter abbreviated to "6P"), pentaporphyrin (hereinafter abbreviated to "5P"), coproporphyrin I (hereinafter abbreviated to "CPI") isomer, mesoporphyrin (hereinafter abbreviated to "Meso"), uroporphyrin III (hereinafter abbreviated to "UPIII"), and coproporphyrin III (hereinafter abbreviated to "CPIII"). Acetonitrile was used for HPLC. The other reagents used were all special-grade reagents.

2. Samples

ALA hydrochloride (1 g) was dissolved in 5% glucose (50 mL) and orally administered to 8 volunteers (7 males and 1 female). Four hours later, samples obtained by blood and urine collection were used. In addition, in the case of one patient diagnosed as having a brain tumor (glioblastoma IV), a preparation provided by Dr. Utsugi from Kitasato University was used.

3. Preparation of samples

An ethyl acetate-acetic acid mixed solution (4/1, v/v) (800 μ L) was added to each plasma sample (200 μ L), followed by mixing with a vortex mixer and centrifugation at 15,000 rpm for 5 minutes. After centrifugation, the supernatant was collected and dried by nitrogen purge and then mixed with a methanol-acetic acid mixed solution (1/1, v/v) (100 μ L). The obtained mixture (40 μ L) was injected into an HPLC.

A 0.08% iodine-acetic acid mixed solution (1/1, v/v) (200 μ L) was added to each urine sample (200 μ L), followed by mixing with a vortex mixer and centrifugation at 15,000 rpm for 5 minutes. After centrifugation, the supernatant (40 μ L) was collected and injected into an HPLC.

4. HPLC analysis conditions

The system used was Shimadzu LC-10A VP. The column used was Shiseido CAPCELL PAK C18 AG120. The detector used was RF-10AXL fluorescence detector (Ex. 406 nm, Em. 609 nm). For the mobile phase, solution A (12.5% acetonitrile-1 M ammonium acetate liquid mixture (pH 5.15)) and solution B (80% acetonitrile-50 mM ammonium acetate liquid mixture (pH 5.15)) were used. The gradient conditions were as follows: 5-minute hold with solution A, linear gradient of A/B (100/0)-A/B (65/35) for 35 minutes, linear gradient of A/B (65/35)-A/B (0/100) for 1 minute, 9-minute hold with solution B, linear gradient of A/B (0/100)-A/B (100/0) for 1 minute, and 9-minute hold with solution A. Determination was carried out at a flow rate of 1.0 ml/min and a temperature of 40°C.

Results

1. Examination of HPLC analysis conditions

A standard porphyrin solution was dissolved by adding 2.4N HCl (0.2 mL) to a Kit, followed by sonication for dissolution. Thereafter, the resultant was washed with 50% acetic acid (approximately 5 mL) in a 10-mL measuring flask. UPIII and CPIII were each accurately weighed to 1 mg, followed by the addition of 2.4N HCl (10 mL) and sonication for dissolution. Thereafter, the obtained resultants were separately measured with 50% acetic acid (20 mL). Thus, a UPIII standard solution (55.329 nmol/mL) and a CPIII standard solution (68.715 nmol/mL) were obtained. The UPIII standard solution and the CPIII standard solution (in an amount corresponding to 10 nmol) were added to the Kit. The total volume was adjusted to 10 mL with 50% acetic acid so that a standard stock solution containing each porphyrin at a concentration of 1,000 nmol/L was prepared. This stock solution (40 μ L) was injected into the column, followed by comparison with the HPLC method by Kondo (Fig. 1). It was found that all

porphyrins including isomers can be separated using the method of this study. Next, in order to confirm the quantification performance of this method, a dilution linearity test, a within-run reproducibility test, and a recovery test were conducted.

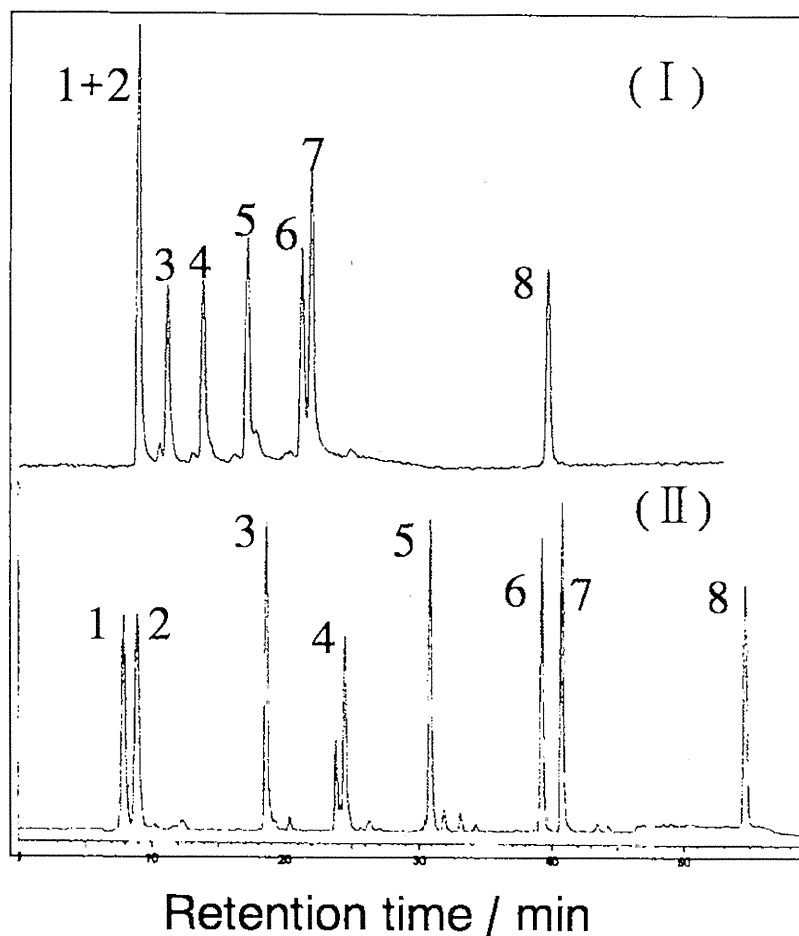


Fig1. Comparison between conventional method and New method

(I) Conventional method (This method by Kondo) , Mobile phase use A sol(80% Acetonitrile,7 % Acetic acid 50mM Ammonium acetate) and B sbo(10% Acetonitrile,4 % Acetic acid, 50mM Ammonium acetate), (II) New mehod and Standard solution is shown 1,Uroporphyrin I ; 2, UroporphyrinIII ; 3,7P ; 4,6P ; 5,5P ; 6,Coproporphyrin I ; 7,Coproporphyrin III ; 8,Mesoporphyrin.

In the dilution linearity test, the standard stock solution was added to plasma from a healthy volunteer. A prepared plasma sample containing each porphyrin at a concentration of 50 nmol/l was subjected to predetermined pretreatment. The obtained methanol-acetic acid solution was diluted 2-, 4-, and 8-fold with a 50% acetic acid

aqueous solution. Each diluted solution (20 μ l) was injected into an HPLC.

Then, each porphyrin level was determined based on the calibration curve and was plotted so as to obtain dilution linearity. As a result, in each case, the correlation coefficient was $r = 0.995$ or more. Preferable straight lines were created based on 8 types of porphyrin samples prepared with the use of plasma (Fig. 2). Also in the case of urine, the correlation coefficient was $r = 0.995$ or more. Accordingly, preferable straight lines were created (data omitted).

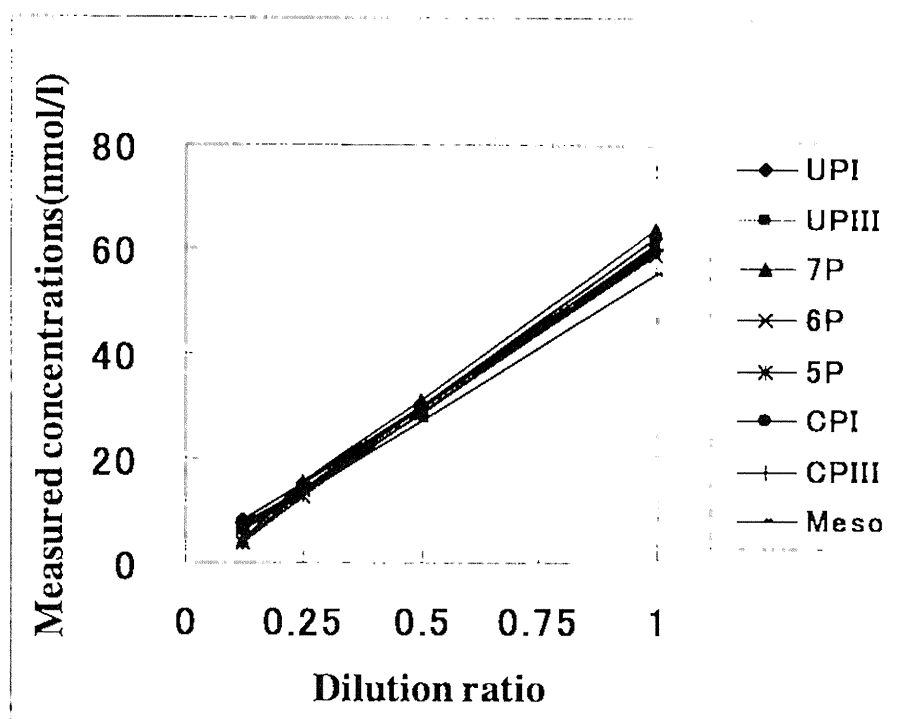


Fig2. Linearity of dilution curves using plasma sample

For the within-run reproducibility test, the urine sample used was prepared by adding each porphyrin so as to result in 400 nmol/l to pooled urine from a healthy individual. In addition, the plasma sample used was prepared by adding each porphyrin so as to result in 50 nmol/l to plasma from a healthy individual.

Determination was carried out 5 times with the use of the plasma and urine samples. As a result, the variation coefficient was found to be 3.4% to 4.1% in urine and 0.6% to 4.6% in plasma. A good variation coefficient of $CV = 5\%$ or less was confirmed in both cases (Tables 1 and 2).

Table1 Within-run reproducibility of Porphyrins in Urine

	average(nmol/l) (n = 5)	SD(nmol/l) (n = 5)	CV(%) (n = 5)
UP I	363	13	3.6
UP III	428	14	3.4
7P	367	15	4.1
6P	374	13	3.4
5P	377	13	3.4
CP I	381	13	3.4
CP III	343	12	3.5
Meso	345	14	3.9

Table2 Within-run reproducibility of Porphyrins in Plasma

	average(nmol/l) (n = 5)	SD(nmol/l) (n = 5)	CV(%) (n = 5)
UP I	51.2	1.2	2.4
UP III	48.5	1.3	2.6
7P	54.0	2.4	4.5
6P	53.2	2.0	3.8
5P	52.7	1.5	2.8
CP I	53.4	0.3	0.6
CP III	47.9	2.2	4.6
Meso	51.5	2.1	4.1

For the recovery test, the sample used was prepared by adding a standard stock solution or purified water (1 volume) containing each porphyrin at a concentration of 500 nmol/l to pooled urine or plasma from a healthy volunteer (9 volumes).

The recovery rate was calculated by the following equation.

Recovery rate (%) = $\frac{(\text{determination value from urine or plasma} + \text{standard stock solution}) - (\text{determination value from urine or plasma} + \text{purified water})}{50} \times 100$

Accordingly, CPI and CPIII were present in base urine and base plasma. Meanwhile, the recovery rate was from 82% to 103% in urine and from 93% to 108% in plasma. A good recovery rate of $\pm 20\%$ or less was confirmed (Tables 3 and 4).

Based on the above results, it has been confirmed that it is reasonable to use the method of this study as a method for determining 8 types of porphyrins in human urine or plasma.

Table3 Recovery of Porphyrins in Urine

	Endogenous porphyrins (nmol/l)	Additive amount (nmol/l)	Measured concentrations	Recovery (%)
UP I	0.0	50.0	51.7	103.4
UP III	0.0	50.0	51.1	102.0
7P	0.0	50.0	51.4	103.0
6P	0.0	50.0	51.2	102.0
5P	0.0	50.0	50.8	102.0
CP I	9.5	50.0	58.6	98.5
CP III	50.8	50.0	91.8	91.1
Meso	0.0	50.0	42.3	84.6

Table4 Recovery of Porphyrins in Plasma

	Endogenous porphyrins (nmol/l)	Additive amount (nmol/l)	Measured concentrations	Recovery (%)
UP I	0.0	50.0	51.2	102.4
UP III	0.0	50.0	48.5	97.0
7P	0.0	50.0	54.0	108.0
6P	0.0	50.0	53.2	106.4
5P	0.0	50.0	52.7	105.4
CP I	1.6	50.0	53.4	103.5
CP III	1.4	50.0	47.9	93.2
Meso	0.0	50.0	51.5	103.0

2. Significance of determination of porphyrins in plasma from human volunteers and plasma from brain tumor patients

One brain tumor patient was compared with 8 healthy adult volunteers. ALA was administered to the patient and the volunteers. Before and 4 hours after ALA administration, the porphyrin concentrations in plasma and urine were determined. Before ALA administration, UPI, UPIII, CPI, and CPIII levels in plasma and urine were high in the brain tumor patient. However, no significance was confirmed. Meanwhile, 4 hours after ALA administration, the CPIII concentration (approximately 4 times greater than that in the volunteers) in urine and the UPI concentration (approximately 3.5 times greater than that in the volunteers) and the UPIII concentration (approximately 1.5 times greater than that in the volunteers) in blood were significantly higher in the brain tumor patient than that in the volunteers. A high CP concentration in urine or a high UP concentration in blood after 5-ALA administration indicates the presence of a lesion exhibiting hypermetabolism of 5-ALA in the body. Therefore, the above results suggest that porphyrin concentrations can be used as a tumor marker.

IV. Discussion

For porphyrin determination in plasma or urine, the HPLC method by Kondo has been used. However, it has been verified that using the method of this study allows confirmation of porphyrins including isomers as shown in Fig. 1. The method of this study is an improved method by which isomers can be separated by gradient of the salt concentration (from a high concentration to a low concentration) in an acetonitrile-based eluent. Hitherto, there have been no findings concerning such method. In addition, it has been verified that quantification in terms of recovery rate and reproducibility can be achieved by this method for daily tests with sufficient accuracy. In this method, protoporphyrin IX (hereinafter abbreviated to "PPIX") was quantified from a Meso standard substance. However, it will be also necessary to examine the reproducibility and the recovery rate by this method with the addition of PPIX as a standard substance instead of Meso.

In addition, in this study, we found that porphyrins can be used as a tumor marker by determining porphyrins in plasma or urine obtained from healthy volunteers and cancer patients before and after ALA administration and determining porphyrins in plasma or urine after ALA administration. However, we were unable to elucidate the reason that the CP concentration in urine and the UP concentration plasma become high. There is probably a mechanism related to porphyrin clearance in nephrons. For example, it is necessary to examine affinity between generated plasma protein or albumin and porphyrin. This is a future objective to be examined.

- 1) Shu-ichiro Ogura, Masahiro Ishizuka, Yasuhiro Mizokami, Kanako Honda, Kenji Tabata, Toshiaki Kamachi, Tohru Mochizuki and Ichio Okura., Analysis of porphyrins in mouse plasma after administration of 5-aminolevulinic acid as a potential tumor marker. *Porphyryns.*, 18, 25-30(2009).
- 2) Masao Kondo, Masahito Aminaka, Toshiaki Tanaka, Iwao Nakamura and Yoshiro Kudo, Rapid procedure for plasma porphyrin assay and clinical significance. *Porphyryns.*, 5, 349-355(1996).
- 3) Masao Kondo., A new developmet of the method of uroporphyrinogen III synthase activity and its clinical significance. *Porphyryns.*, 1, 51-57(1992).

- 4) Masao Kondo., Rapid Procedure for fecal porphyrin assay ad it's clinical significance. *Porphyrius.*, 2, 85-91(1993).

トピックス

遺伝子発現調節のリガンドとしてのヘムの機能

Heme-dependent Regulation of Gene Expression and Protein Functions

ヘムはヘムタンパク質の補欠分子族として、ガス分子の輸送や酸化還元反応を始めとする種々の酸素反応を担うことが知られてきたが、近年、タンパク質の機能を調節するリガンドとしてのヘムやガスセンサーとしての機能が知られるようになり、新たなヘムの機能を解明する研究が展開されている。ヘムは鉄とプロトポルフィリンIXの複合体として知られており、地球のほとんどの生物において存在して、好氣的な生命機能の維持に関与することが知られている。ヘムの研究は医薬学、農学、工学をはじめとする種々の分野で行われており、ほ乳動物では肝臓や赤血球におけるヘム合成や分解について詳細な研究がされてきた。

動物のヘム合成の初発段階はミトコンドリアのグリシンとスクシニル-CoAの縮合に始まる8段階の酵素反応によって進行し、それらの4段階の反応に関与する酵素は細胞質に、残りの反応に関与する酵素はミトコンドリアに局在している¹⁾。ヘム合成の律速段階は、初発酵素の δ -aminolevulinic acid synthase (ALAS)である。またヘム合成には鉄イオンが必要であり、小腸から取り込まれた鉄分子は血液中を移動して主に各組織細胞の表面にある transferrin receptor を介して細胞内に取り込まれる。生体内でのヘム鉄の維持に最も大きなウエイトを占めるのは十二指腸からの鉄イオンの取り込みであり、食事の鉄不足は細胞の鉄やヘムの低下をもたらす²⁾。

生体内の鉄利用に重要な役割を果たしているのはヘム分解を行う heme oxygenase (HO) である。HO は NADPH-cytochrome P450 reductase, NADPH および分子状酸素を使ってヘムを酸化的に分解する。本反応の生成物のひとつビリベルジンは直ちに biliverdin reductase によってビリルビンになって排泄される。また、HO は鉄イオンと一酸化炭素 (CO) を生成し、鉄イオンは再利用され、CO はストレス弛緩物質としての機能を果たすことが知られるようになった³⁾。HO は HO-1 と HO-2 の2種類のアイソザイムがあり、HO-1 は酸化的ストレス、金属、熱、炎症やサイトカインなどの種々の因子と基質であるヘムによって誘導されるストレスタンパク質である⁴⁾。一方、HO-2 の発現は一定で、特に神経細胞や精巣細胞での発現量が多い。HO の大きな役割には hemoglobin を始めとするヘムタンパク質の鉄イオンの再利用である⁵⁾。HO-1 欠乏マウスでは極度の貧血とマクロファージなどでの顕著な鉄

の蓄積が認められることからヘム分解の多くは HO-1 が行っていることが伺える。従って、ヘム鉄の行方は HO-1 に依存する鉄イオンの細胞外への放逐と HO-1 に依存しない遊離鉄の維持の二通りがあると考えられる⁴⁾。

細胞内ヘムレベルのヘムによる調節

ALAS には広く種々の組織に発現する ALAS1 と赤血球系細胞で働く ALAS2 の2種類のアイソザイムが知られており²⁾、それぞれ違った調節を受けている。ALAS1 発現はヘムによって負のフィードバック調節を受け細胞内のヘム量の維持に重要な役割を果たしている。ALAS1 のヘムによる抑制は転写、ALAS1 mRNA のヘムによる不安定化さらには翻訳後の ALAS1 前駆体のミトコンドリアへの局在の抑制に及ぶ(図1)。ALAS1 前駆体の移行のヘムによる抑制は ALAS1 前駆体のミトコンドリア局在部位の heme-regulatory motif (HRM) に相当するシステイン-プロリンを含む K/RCPV アミノ酸配列 (CP-motif) へのヘムの会合によるものである⁶⁾。ALAS1 mRNA への転写調節については、長年多くの研究がなされてきて、ヘムによる抑制の他に種々の薬剤やアルコールを始めとするいろいろな因子での誘導が知られ、数種類の核因子が遺伝子発現を調節することが知られている⁷⁾。しかし、ヘムによる ALAS1 の転写抑制については明確な機構の解明には至っていない。最近、ほ乳動物で核因子 REV-erba がヘムを結合して、ALAS1 のエンハンサー領域の E-box に結合して活性化因子 PGC-1 α を排除して Co-repressor である抑制因子 NCOR-REV-erba 複合体が ALAS1 遺伝子を不活性化するのではないかと考えられている⁸⁾。我々はマウス ALAS1 遺伝子のヘムによる転写抑制について詳細に調べた結果、ヘミン (20-50 μ M) 処理した細胞では ALAS1 遺伝子の近位プロモーター領域 (-300bp 付近) の GC-rich 配列に転写因子 EGR-1 が結合することを見出した。EGR-1 はさらに抑制因子 NAB1/2 と複合体を形成して遺伝子を不活性化するが、ヘムがこれらの因子とどのような相互作用をするかは不明である⁹⁾。

ヘムによる HO-1 発現の顕著な誘導は細胞内のヘムレベルを低下させることに貢献する。種々のストレスで誘導される HO-1 遺伝子のプロモーター領域には種々の調節因子が結合することが知られている⁴⁾。ヘムによる遺伝子の活性化については全てのことが明らかにされてい

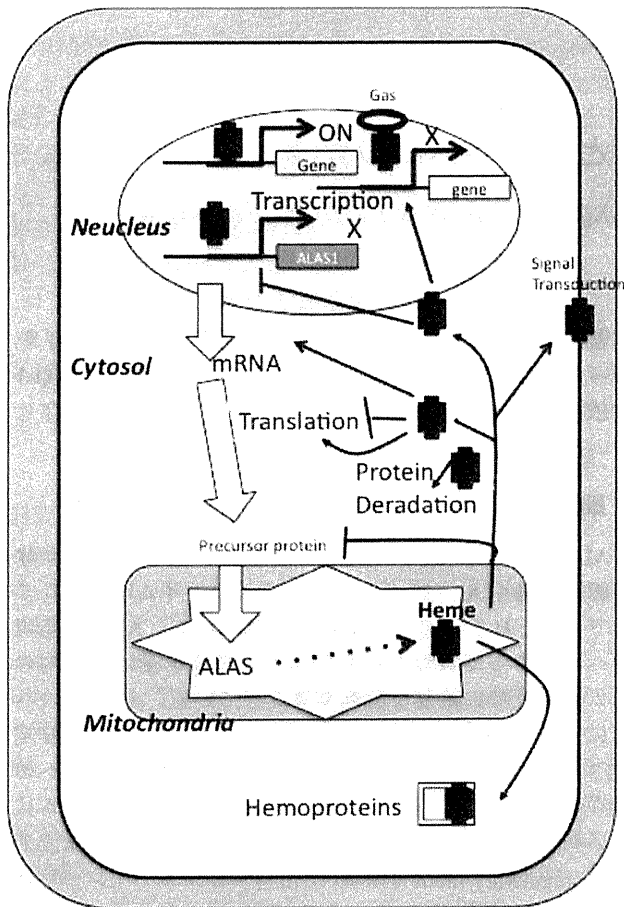


図1. ヘム合成調節メカニズムとヘムの多極的利用とその作用

るわけではない。しかし、近年、抑制因子 Bach1 にヘムが結合すると Bach1 の抑制活性が失われることで HO-1 の誘導が説明できるようになった。すなわち、Bach1 は Maf 因子と複合体を形成して HO-1 遺伝子の転写開始点から 10kb 以上上流にある MARE 部位に結合して遺伝子発現を抑制しているが、ヘムと結合することによって MARE 部位から離脱して代わりに活性化因子 NRF2 が Maf 因子と複合体を形成して MARE 部位に結合して遺伝子を活性化すると考えられている¹⁰⁾¹¹⁾。

分化因子としてのヘム

ヘムは種々の細胞分化を促進することは以前から多くの報告がある。最もよく知られているのは赤芽球細胞の分化時のヘムの必要性である。赤芽球分化段階の細胞群のひとつである colony-forming unit (CFU) に関して、分化因子エリスロポエチンが存在してもヘム合成を阻害すると CFU の段階で分化の停止がみられ、またヘミンを添加すると CFU 細胞の増加が認められることが報告されている¹²⁾。マウス赤白血病 (MEL) 細胞はジメチルスルホキシド等の有機溶剤処理で赤血球様に分化することがよく知

られている。この細胞をヘミン (20-100 μM) で処理すると同様にヘモグロビン合成は誘導されて分化することが知られている¹³⁾¹⁴⁾。これらの処理によって細胞内のヘム合成系酵素を始め種々のヘム依存性の赤芽球特異的タンパク質が誘導されていると考えられる (後述)。

マウス線維芽細胞 3T3-L1 をインスリンとデキサメサゾン等のホルモンで処理すると脂肪細胞に分化することが知られているが、この細胞をヘミン (25 μM) で処理すると同様に分化することが報告されており¹⁵⁾、さらにラット筋肉細胞でも同様な分化が認められている¹⁶⁾。また、ヒトの神経芽腫細胞をヘミン (50 μM) 処理した結果、神経特異的タンパク質の誘導や神経軸の成長が認められたことが報告されている¹⁷⁾¹⁸⁾。これらの細胞分化時には組織特異的な遺伝子が活性化されていると考えられる。一方、細胞によってはヘミン処理をするとミトコンドリア DNA の破壊などの細胞毒をもたらすことが多く報告されており¹⁹⁾、生体外の実験系がもたらす問題としてヘム毒も考慮しなければならない。

ヘム依存性の遺伝子発現

核内のヘムによって転写が支配されていることが最初に知られるようになったのは酵母のミトコンドリア呼吸鎖のタンパク質である iso-1-cytochrome (CYC1) と iso-2-cytochrome (CYC2) である。すなわち、好気条件下で生育すると iso-1-cytochrome のみが産生される。CYC1 と CYC2 は活性化因子 HAP1 がプロモーター領域 (UAS1) に結合することで活性化される。HAP1 の UAS1 への結合はヘムによって増加する。HAP1 は DNA に結合するジンクフィンガー領域とヘムに結合する CP-motif を含む活性化部位から構成されている²⁰⁾。ヘム-HAP1 関与で転写が促進する他の遺伝子として COXVb, cytochrome b₂, catalase T と CPOX などが知られているが、COXVa は逆に同様な様式で抑制される²⁵⁾。光合成細菌を始めとする多くのバクテリアではヘム結合調節因子 CooA が同定され、CO を配位して始めてゲノムに結合して遺伝子を活性化することが知られるようになり、現在もっともよく研究されたガスセンサーである²¹⁾。

ほ乳動物で最初にヘム結合性を有する転写因子として発見されたのは Bach1 であり、Maf 因子と会合する遺伝子抑制因子である。Bach1 には 6 箇所 CP-motif が存在しており、ヘムが Bach1 の CP-motif に結合すると抑制因子としての活性を低下させることが知られるようになった。赤血球分化にともなって α , β -globin が誘導されるが、その時、活性化因子 NF-E2-Maf 複合体が globin 遺伝子のエンハンサー領域 (μLCR) にある MARE サイトに結合して遺伝子を活性化することが証明されている²²⁾²³⁾。同様に MARE サイトを認識する Bach1-Maf の抑制活性をヘムが取り除くことで、NF-E2 を引き寄せて globin 発現を引き出していると考えられている。Bach1 の機能としては

前述の非赤芽球系細胞でのHO-1のヘムによる誘導の場合と類似の機構であるといえる¹⁰⁾。しかし、ヘムが生体のglobin産生に必須であるということに関しては、否定的な見解も多い。実際、ヘムを少量しか合成できない変異赤血球でもglobin mRNAレベルは正常であるということからも伺える。ヘムを活性化因子とする遺伝子発現は、薬剤代謝を担うフェノバルビタール誘導性のcytochrome P-450 (b型)の増加には遺伝子プロモーター領域へのヘム結合ファクターの結合が報告されているが、因子の同定までには至っていない²⁴⁾。

2005年、ショウジョウバエの核因子E75がヘムを結合する能力があつてエクザイゾンシグナルに関与すると考えられる標的遺伝子のプロモーター領域に結合して転写を抑制するが、CO/NO等のガスが配位するとco-activatorが結合して遺伝子を活性化することが報告され、核因子のリガンドとしてのヘムが知られるようになった²⁵⁾。ほ乳動物でもE75にホモロジーのある核因子REV-erb α (前出)がヘムを結合して、plasminogen activatorやALAS1を始めとする種々の遺伝子のRORE様エンハンサー領域に結合して活性化因子PGC-1 α やPPAR γ の結合部位と競合するとも考えられる⁸⁾。しかし、REV-erb α はE75のホモログであり、E75ではヘムにCOやNOが配位することが知られているので²⁶⁾、今後REV-erb α 結合ヘムへのガスの配位による分子機能の調節機構が明らかにされる必要がある。また、ヘム産生には概日周期があり、その変化は細胞内ヘムレベルの変化によるALAS1の発現量の変動に起因していることが示された²⁷⁾。ALAS1の概日周期下の発現調節には時計遺伝子NPAS2がヘムに結合してBMAL1と複合体を形成することでALAS1遺伝子を活性化するが、COがNPAS2/BMAL1複合体の活性を抑制することが分かり、NPAS2はガスセンサーとしての役割が明らかにされた。COはHOの反応産物であるので、細胞内のヘムレベルの上昇に伴ってCOが増加してALAS2遺伝子の不活性化を行う合理的なフィードバック調節が考えられている。さらに、NPAS2/BMAL1複合体を活性化する時計因子PER2もまたヘムが結合する部位を2個有しており、その一方に酸化型ヘムが結合すると不安定になって分解されるが、2個のヘムもしくは還元型ヘムと時計因子CRYが結合すると安定化されて標的遺伝子のプロモーターに結合して遺伝子発現活性を促進すると考えられている。これらの結果からPER2はヘムセンサーとも言われるようになった。このような調節はALAS1の他に、赤血球系のALAS2遺伝子を概日周期によって制御されるE-Boxをプロモーターに持つ遺伝子群の発現において同様な機構で調節されていることが明らかにされてくるに至り、さらにヘムの新しいリガンドとしての機能が注目されることになった^{28),29)}。以上のように、ヘムは酸素やCOを配位してタンパク質機能を変化させて標的遺伝子の発現を調節していることからガスセンサーの主

役といわれるようになった。

ヘム結合性核因子REV-erb α はマウス3T3-L1脂肪細胞の分化時に誘導されることが報告され³⁰⁾、ヘムによる脂肪細胞の分化の促進と関係すると考えられた。我々は数種類の核因子のヘム結合性を調べたところ、脂肪細胞分化の中心的役割を果たすRXR α にヘム結合能力があることを見出した。しかし、ヘムはRXR α の機能を低下させて3T3-L1細胞の分化を抑制することが分かった³¹⁾。ほ乳動物におけるヘムと調節因子の相互作用に関しては、抑制因子の機能を低下される場合のみが報告されており、未だHAP1のようにヘムによって直接活性化される転写因子は発見されていない。

転写後のヘムによる機能制御

赤芽球細胞でのグロビンなどのタンパク質合成を調節するprotein kinaseの活性はヘムによって調節され、heme-regulated inhibitor (HRI)と呼ばれている。HRIはeIF2 α の α サブユニットをリン酸化して翻訳を阻害する。eIF2 α のリン酸化はHRI, double strands RNA-dependent kinase, GCN-2, ER resistant kinaseなどで行われているが、HRIのみがヘムと結合することによってkinase活性を低下させる。従って、HRI活性の低下はeIF2 α を活性化し、赤芽球の主要タンパク質グロビンの合成を増加させることが知られている。HRIの活性低下はALAS2の翻訳をも促進し、hemoglobin合成促進の相乗効果を生む³²⁾。最近、ヘムによる転写後の調節についても種々のステップでみられることが報告されるようになった。microRNA前駆体の成熟過程にはDGCR8の関与が必須であるが、ヘムが結合したDGCR8の二量体がmicroRNA前駆体と複合体を形成するという興味深い調節が最近報告された³³⁾。しかし、その詳細は検討されておらず、今後の進展を期待したい。

細胞内の遊離鉄イオンは遊離ヘムと同様に毒性が高く、鉄レベルは細胞への鉄の取り込み、利用、貯蔵および排出で厳密に調節されている。これらの鉄の動態を調節するタンパク質群のmRNAにはiron-responsive element (IRE)が存在しており、IRE結合タンパク質 (IRP)の部位への結合と解離で調節されている。IRPは2種類のアイソホム (IRP1と2)が知られている。IRP1は鉄-イオウクラスター含有タンパク質でaconitase活性を示すが、クラスターの完成度と逆の相関でmRNA内のIREとの結合能を獲得する。IRP2のIREの結合量はその量的な変動で調節されている。IRP2はプロテオソームで分解されるが、鉄レベルの増加でIRP2の酸化が自らのユビキチン化を招いて分解される。IRP2の酸化にはIRP2のiron-dependent degradation (IDD)部位への酸化型ヘムの関与が必要であり、IDD部位のE3 ligaseの認識機構にヘム結合タンパク質HOILが必要であることが報告されている³⁴⁾。しかし、IDD部位とHOILが関与する鉄依存性のIRP2の分解につ

いて疑問視する報告があり³⁵⁾、さらに、最近鉄結合部位 hemerythrin 様配列を有する FXBL5 が IRP2 の鉄依存性分解に作用することが知られるようになり³⁶⁾、細胞内鉄イオンレベルは多極的に調節されている可能性も考えられる興味深い問題である。

ヘム輸送体として動物で最初に単離されたのは FLVCR である。FLVCR は猫の白血病ウイルスの細胞表面抗原であることが知られていた。近年、その機能としてはヘムの細胞外輸送 (exporter) として働いていると考えられるようになり、FLVCR ノックアウトマウスでは脾臓や血球細胞に顕著な鉄の蓄積が認められることからマクロファージのヘムの細胞外輸送に関与することが分かった³⁷⁾。HRG-1 もヘム輸送体として知られ、エンドゾームに局在して H⁺-ATPase に会合し、エンドゾームを酸性 pH に維持して鉄の取り込みに関与する transferrin receptor を始めとする栄養輸送体のエンドサイトーシスに働くと考えられている。HRG-1 は本来ヘム合成が欠損している線虫においてヘム獲得のためのタンパク質として分離されており、動物やゼブラフィッシュにおいてもホモログが存在し、赤血球産生には必要な膜タンパク質であることが知られている³⁸⁾。また、細胞内への鉄の取り込みは 2 価鉄を輸送する divalent metal transporter (DMT) が担っているが、細胞表面では 3 価鉄を 2 価鉄に還元する必要がある。鉄イオンの還元には膜貫通型の cytochrome b₅₆₁ ファミリーのヘムタンパク質 Dcytb が知られるようになり、Dcytb は特に小腸での 2 価鉄の取り込みには必須である。cytochrome b₅₆₁ ファミリーには 101F6, SDR2 を始めとする機能不明の膜貫通型のヘムタンパク質が知られており、それらはアスコルビン酸の産生と共役して種々の低分子物質の化合物の還元反応に関与している可能性が考えられる³⁹⁾。一方、赤芽球系には鉄含有膜タンパク質 Steap3 が鉄イオンの還元に関与していることが知られている⁴⁰⁾。また、生体膜の透過性に働くイオンチャネルのうちでジストロフィン依存性筋ジストロフィーに関連するカルシウム依存性 Slo1 BK チャネルは、保存されたヘム結合配列モチーフを有している。ヘムがヒト Slo1 チャネルおよびラットの脳にある野生型 BK チャネルを直接制御しているということが電気生理学的・構造学的な証拠によって示された。すなわち、酸化型と還元型のヘムが Slo1 チャネルタンパク質に結合して、チャネル開口頻度を減らすことにより膜透過 K⁺ 電流を著しく阻害する。この BK チャネルの直接制御により、これまで知られていなかった急性のシグナル伝達分子としてのヘムの役割が明らかになった⁴¹⁾。

近年、種々のヘム結合タンパク質やヘム輸送タンパク質の発見が相次いでおり、それぞれのヘム利用は興味深い。HCP-1, OXG, ABCG2 などはヘムやポルフィリンの輸送に関係すると報告されているが、それらの機能には曖昧な点のあることが指摘されている。さらに、in

vitro での実験が生み出す artifact の可能性もあり、本来の機能解明にはまだまだ多くの検証が必要である。ヘムが可逆的にタンパク質に配位して機能を変換させ、また様々なガスのセンサーとして働いて細胞機能を緻密に調節することが、種々の遺伝病や変異生物の原因分子の性質の解明から明らかにされてきている。今後、さらなるヘムを始めとする小分子による機能制御の研究の発展が原因不明の疾病の解明につながることを期待してやまない。

Key Words : heme, transcription, nuclear receptor, heme oxygenase, ALAS1

Department of Biotechnology, Kyoto Institute of Technology

Shigeru Taketani

京都工芸繊維大学応用生物学部門 竹谷 茂

文 献

- 1) 古山和道, 佐々 茂 (2003) ヘム合成と鉄代謝. 生化学 **75**, 179-186
- 2) Taketani S (2005) Acquisition, mobilization and utilization of cellular iron and heme: endless findings and growing evidence of tight regulation. *Tohoku J Exp Med* **205**, 297-318
- 3) Shibahara S (1988) Regulation of heme oxygenase gene expression. *Semin Hematol* **25**, 370-376
- 4) Kikuchi G, Yoshida T, Noguchi M (2005) Heme oxygenase and heme degradation. *Biochem Biophys Res Commun* **338**, 558-567
- 5) Maines MD (1997) The heme oxygenase system: a regulator of second messenger gases. *Annu Rev Pharmacol Toxicol* **37**, 517-554
- 6) Lathrop JT, Timko MP (1993) Regulation by heme of mitochondrial protein transport through a conserved amino acid motif. *Science* **259**, 522-525
- 7) Podvinez M, Handschin C, Looser R, Meyer UA (2004) Identification of the xenosensors regulating human 5-aminolevulinic synthase. *Proc Natl Acad Sci USA* **101**, 9127-9132
- 8) Wu N, Yin L, Hanniman EA, Joshi S, Lazar MA (2009) Negative feedback maintenance of heme homeostasis by its receptor, Rev-erb α . *Genes Dev* **23**, 2201-2209
- 9) Gotoh S, Nakamura T, Kataoka T, Taketani S (2009) Possible involvement of EGR-1 in transcriptional regulation of the mouse ALAS1 gene by heme. 第 32 回日本分子生物学会年会 (横浜 2009.12) 要旨集 2P-0231.
- 10) Sun J, Hoshino H, Takaku K, Nakajima O, Muto A, Suzuki H, Tashiro S, Takahashi S, Shibahara S, Alam J, Taketo MM, Yamamoto M, Igarashi K (2002) Hemoprotein Bach1 regulates enhancer availability of heme oxygenase-1 gene. *EMBO J* **21**, 5216-5224
- 11) Alam J, Igarashi K, Immenschuh S, Shibahara S, Tyrrell RM (2004) Regulation of heme oxygenase-1 gene transcription: recent advances and highlights from the International Conference (Uppsala, 2003) on Heme Oxygenase. *Antioxid Redox Signal* **6**, 924-933
- 12) Gilmore MM, Bishop TR (1999) The role of c-myb during the maturation of murine CFU-E. *Blood Cells Mol Dis* **25**, 68-77

- 13) Fukuda Y, Fujita H, Taketani S, Sassa S (1993) Dimethyl sulphoxide and haemin induce ferrochelatase mRNA by different mechanisms in murine erythroleukaemia cells. *Br J Haematol* **83**, 480-484
- 14) Sassa S, Nagai T (1996) The role of heme in gene expression. *Int J Hematol* **63**, 167-178
- 15) Chen JJ, London IM (1981) Hemin enhances the differentiation of mouse 3T3 cells to adipocytes. *Cell* **26**, 117-122
- 16) Swierczewski E, Pello JY, Arapinis C, Aron Y, Krishnamoorthy R (1987) Characterization of rat preadipocytes from normal rat adipose tissue by their effector response. *Biochem J* **248**, 383-387
- 17) Ishii DN, Maniatis GM (1978) Haemin promotes rapid neurite outgrowth in cultured mouse neuroblastoma cells. *Nature* **274**, 372-374
- 18) Bonyhady RE, Hendry IA, Hill CE, McLennan IS (1982) Effects of haemin on neurones derived from the neural crest. *Dev Neurosci* **5**, 125-129
- 19) Kumar S, Bandyopadhyay U (2005) Free heme toxicity and its detoxification systems in human. *Toxicol Lett* **157**, 175-188
- 20) Pfeifer K, Kim KS, Kogan S, Guarente L (1989) Functional dissection and sequence of yeast HAP1 activator. *Cell* **56**, 291-301
- 21) Gilles-Gonzalez MA, Gonzalez G (2005) Heme-based sensors: defining characteristics, recent developments, and regulatory hypotheses. *J Inorg Biochem* **9**, 1-22
- 22) Ogawa K, Sun J, Taketani S, Nakajima O, Nishitani C, Sassa S, Hayashi N, Yamamoto M, Shibahara S, Fujita H, Igarashi K (2001) Heme mediates derepression of Maf recognition element through direct binding to transcription repressor Bach1. *EMBO J* **20**, 2835-2843
- 23) Tahara T, Sun J, Nakanishi K, Yamamoto M, Mori H, Saito T, Fujita H, Igarashi K, Taketani S (2004) Heme positively regulates the expression of beta-globin at the locus control region via the transcriptional factor Bach1 in erythroid cells. *J Biol Chem* **279**, 5480-5487
- 24) Sultana S, Nirodi CS, Ram N, Prabhu L, Padmanaban G (1997) A 65-kDa protein mediates the positive role of heme in regulating the transcription of CYP2B1/B2 gene in rat liver. *J Biol Chem* **272**, 8895-8900
- 25) Reinking J, Lam MM, Pardee K, Sampson HM, Liu S, Yang P, Williams S, White W, Lajoie G, Edwards A, Krause HM (2005) The Drosophila nuclear receptor e75 contains heme and is gas responsive. *Cell* **122**, 195-207
- 26) Marvin KA, Reinking JL, Lee AJ, Pardee K, Krause HM, Burstyn JN (2009) Nuclear receptors homo sapiens Rev-erbbeta and Drosophila melanogaster E75 are thiolate-ligated heme proteins which undergo redox-mediated ligand switching and bind CO and NO. *Biochemistry* **48**, 7056-7071
- 27) Okano S, Zhou L, Kusaka T, Shibata K, Shimizu K, Gao X, Kikuchi Y, Togashi Y, Hosoya T, Takahashi S, Nakajima O, Yamamoto M (2010) Indispensable function for embryogenesis, expression and regulation of the nonspecific form of the 5-aminolevulinic synthase gene in mouse. *Genes to Cells* **15**, 77-89
- 28) Kaasik K, Lee CC (2004) Reciprocal regulation of haem biosynthesis and the circadian clock in mammals. *Nature* **430**, 467-471
- 29) Meng QJ, McMaster A, Beesley S, Lu WQ, Gibbs J, Parks D, Collins J, Farrow S, Donn R, Ray D, Loudon A (2008) Ligand modulation of REV-ERBalpha function resets the peripheral circadian clock in a phasic manner. *J Cell Sci* **121**(Pt 21), 3629-3635
- 30) Chawla A, Lazar MA (1993) Induction of Rev-Erba alpha, an orphan receptor encoded on the opposite strand of the alpha-thyroid hormone receptor gene, during adipocyte differentiation. *J Biol Chem* **268**, 16265-16269
- 31) Gotoh S, Ohgari Y, Nakamura T, Osumi T, Taketani S (2008) Heme-binding to the nuclear receptor retinoid X receptor alpha (RXRalpha) leads to the inhibition of the transcriptional activity. *Gene* **423**, 207-214
- 32) Igarashi J, Murase M, Iizuka A, Pichierri F, Martinkova M, Shimizu T (2008) Elucidation of the heme binding site of heme-regulated eukaryotic initiation factor 2alpha kinase and the role of the regulatory motif in heme sensing by spectroscopic and catalytic studies of mutant proteins. *J Biol Chem* **283**, 18782-18791
- 33) Faller M, Matsunaga M, Yin S, Loo JA, Guo F (2007) Heme is involved in microRNA processing. *Nat Struct Mol Biol* **14**, 23-29
- 34) Ishikawa H, Kato M, Hori H, Ishimori K, Kirisako T, Tokunaga F, Iwai K (2005) Involvement of heme regulatory motif in heme-mediated ubiquitination and degradation of IRP2. *Mol Cell* **19**, 171-181
- 35) Zumbrennen KB, Hanson ES, Leibold EA (2008) HOIL-1 is not required for iron-mediated IRP2 degradation in HEK293 cells. *Biochim Biophys Acta* **1783**, 246-252
- 36) Vashisht AA, Zumbrennen KB, Huang X, Powers DN, Durazo A, Sun D, Bhaskaran N, Persson A, Uhlen M, Sangfelt O, Spruck C, Leibold EA, Wohlschlegel JA (2009) Control of iron homeostasis by an iron-regulated ubiquitin ligase. *Science* **326**, 718-721
- 37) Keel SB, Doty RT, Yang Z, Quigley JG, Chen J, Knoblaugh S, Kingsley PD, De Domenico I, Vaughn MB, Kaplan J, Palis J, Abkowitz JL (2008) A heme export protein is required for red blood cell differentiation and iron homeostasis. *Science* **319**, 825-828
- 38) O'Callaghan KM, Ayllon V, O'Keefe J, Wang Y, Cox OT, Loughran G, Forgac M, O'Connor R (2010) The heme binding protein HRG-1 is induced by IGF-I and associates with the Vacuolar (H⁺)-ATPase to control endosomal pH and receptor trafficking. *J Biol Chem* **285**, 381-391
- 39) McKie AT (2008) The role of Dcytb in iron metabolism: an update. *Biochem Soc Trans* **36**(Pt 6), 1239-1241
- 40) Ohgami RS, Campagna DR, Greer EL, Antiochos B, McDonald A, Chen J, Sharp JJ, Fujiwara Y, Barker JE, Fleming MD (2005) Identification of a ferrireductase required for efficient transferrin-dependent iron uptake in erythroid cells. *Nat Genet* **37**, 1264-1269
- 41) Tang XD, Xu R, Reynolds MF, Garcia ML, Heinemann SH, Hoshi T (2003) Haem can bind to and inhibit mammalian calcium-dependent Slo1 BK channels. *Nature* **425**, 531-535

The low expression allele (IVS3-48C) of the ferrochelatase gene leads to low enzyme activity associated with erythropoietic protoporphyria

Tsuyoshi Tahara · Masayoshi Yamamoto ·
Reiko Akagi · Hideo Harigae · Shigeru Taketani

Received: 4 October 2010 / Revised: 8 November 2010 / Accepted: 9 November 2010 / Published online: 4 December 2010
© The Japanese Society of Hematology 2010

Erythropoietic protoporphyria (EPP) is an autosomal-dominant inherited disorder characterized biochemically by the excess accumulation and excretion of protoporphyrin, an intermediate precursor of heme biosynthesis. The enzyme abnormality that underlies protoporphyrin accumulation in EPP is a defect of ferrochelatase (FECH). Patients with EPP are clinically characterized by painful photosensitivity in skin and some (5–10%) exhibit liver failure due to massive hepatic accumulation of protoporphyrin [1, 2]. After we demonstrated the structure of the human *FECH* gene [3], more than 100 different kinds of molecular defects of *FECH* have been reported throughout the world. It has been reported that the low expression of a wild-type allelic variant *trans* to a mutated *FECH* allele is generally required for clinical expression of EPP [4]. According to this background, Gouya et al. [5] have found that the presence of a C at IVS3-48 in the human *FECH* gene causes the low expression of *FECH*. This intronic single nucleotide polymorphism (SNP) of the *FECH* gene, IVS3-48C/T transition, is key to the EPP phenotype. It is suggested that partially aberrant splicing of pre-mRNA by IVS3-48C is responsible for the clinical manifestations of EPP, although change in

the enzyme activity has not been examined. Here, we report mutations of the *FECH* gene associated with IVS3-48C in five Japanese EPP patients. We found that the *FECH* activity of peripheral blood lymphocytes with IVS3-48C/C was <50% of that with IVS3-48T/T suggesting that the variations of the activity in patients with EPP could be based on the different levels of control.

1 Mutation of the *FECH* gene in patients with EPP

We have diagnosed five patients with EPP in Japanese hospitals (Table 1). All patients suffered photosensitivity and three of them (patients 3, 4 and 5) developed hepatic dysfunction and died. Biochemical analysis of all patients showed marked elevation of protoporphyrin in erythrocytes. The *FECH* activity in peripheral blood lymphocytes of EPP patients decreased to 19–39% that of the control. After informed consent for all examinations had been obtained from patients and their families, blood samples were collected for genetic analysis. The total RNA was isolated by the guanidine thiocyanate method from lymphocytes or Epstein–Barr virus-transformed lymphoblastoid cells. cDNAs were synthesized with oligo(dT) primer using ReveTra Ace (Toyobo Co. Ltd., Tokyo, Japan). The entire *FECH* protein-coding region was amplified by PCR using two synthetic primers, 5'-GAGGCTGCCAGGC A-3' and 5'-TTTGCCTAACGCCACGGGGT-3'. The DNA fragments were ligated into pGEM-T vector (Promega Co., Madison, WI). Several plasmids-carrying *FECH* cDNA from a patient were isolated and the inserted DNAs were analyzed by sequencing. We found mutations in cDNAs. To confirm the mutation, we tried to analyze mutations of the *FECH* gene; namely, genomic DNA was isolated from whole blood cells. Regions containing molecular defects

T. Tahara · M. Yamamoto · S. Taketani (✉)
Department of Biotechnology,
Kyoto Institute of Technology,
Kyoto 606-8585, Japan
e-mail: taketani@kit.ac.jp

R. Akagi
Department of Pharmacy, Faculty of Pharmacy,
Yasuda Women's University, Hiroshima 731-0153, Japan

H. Harigae
Department of Hematology and Rheumatology,
Tohoku University Graduate School of Medicine,
Sendai, Miyagi 980-8574, Japan

Table 1 Characterization of Japanese patients with EPP in terms of phenotype and genotype

Patient no.	Sex	Age	Symptoms	Protoporphyrin in blood ($\mu\text{g}/\text{dl}$ RBC)	Mutation in FECH	Genotype of normal allele IVS3-48
1	M	23	Photosensitivity	1,424	IVS4(-4)a>g	C
2	M	33	Photosensitivity	9,274	$\Delta 5\text{b}$ (751-755)	C
3	M	41	Photosensitivity liver failure	12,574	T557C (I186T)	C
4	M	27	Photosensitivity liver failure	8,779	$\Delta 16\text{b}$ (574-589)	C
5	M	36	Photosensitivity liver failure	9,127	IVS9(+1)g>a	C

found in FECH cDNA were amplified with primers as previously reported [6]. The amplified DNAs were directly sequenced. Then, we identified five different mutations that were the same as those previously reported for Japanese and European patients [2]. The common mutations between Asians and Caucasians can be ascribed to their common ancestry.

2 Relation of IVS3-48T/C of the FECH gene to Japanese EPP

The IVS3-48C/T transition of the FECH gene from EPP patients and their families was also analyzed. To amplify the DNA of the intron 3-exon 4 boundary (278 bp), the primers 5'-TCTACAACAAGAGAGCTGGC-3' and 5'-ATCCTGCGGTACTGCTCTTG-3' were used. Five Japanese EPP patients presented in this study were found to exhibit IVS3-48C of the normal allele (Table 1), which is consistent with the previous studies of Japanese [7], Caucasian and Asian EPP patients [2]. On the other hand, all carriers ($n = 4$) in their families were found with IVS3-48T of the normal allele. Other possible low expression alleles of the FECH gene, such as -251 G/A and IVS1-23C/T transitions linked to the disease [4], were also examined for the five EPP families, but the examination was not conclusive. Thus, the variation of IVS3-48C/T transition in the FECH gene may explain the difference in the residual enzyme activities in asymptomatic and symptomatic mutant carriers. Alternatively, because EPP development requires with the mutated allele of the FECH gene as well as the allele with IVS3-48C, it can be said that EPP is a recessive-inherited disease in a broad sense. We examined the relationship of decreased FECH activity with the genotype of the FECH gene, including IVS3-48C/T transition. After the isolation of peripheral blood lymphocytes of EPP patients and Japanese healthy controls, we examined the FECH activity by the formation of zinc-mesoporphyrin [8]; namely, homogenates from lymphocytes were incubated with mesoporphyrin (10 nmol), zinc acetate (40 nmol), Tween 20 (0.01%), and sodium palmitate (400 $\mu\text{g}/\text{mL}$) in 100 mM Tris-HCl, pH 8.0. The formation of Zn-mesoporphyrin was determined by

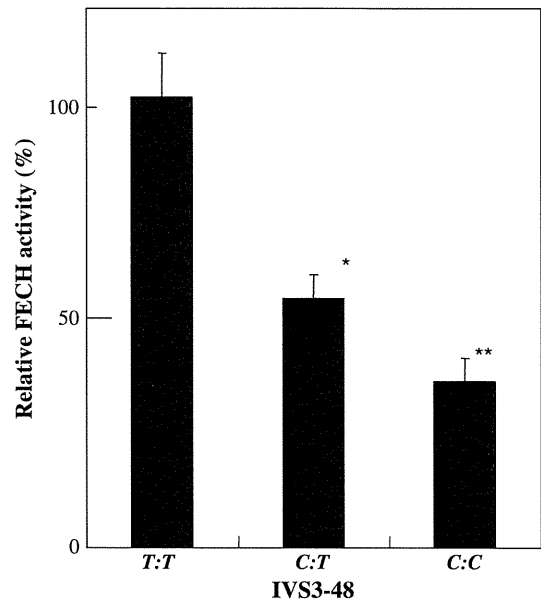


Fig. 1 The FECH activity in peripheral blood T lymphocytes from healthy controls. Lymphocytes were isolated from healthy volunteers with IVS3-48T/T (T:T) ($n = 9$), IVS3-48C/T (C:T) ($n = 10$) and IVS3-48C/C (C:C) ($n = 4$) of the FECH gene. The FECH activity was measured using homogenates. The activity of 100% is equivalent to 67.2 ± 6.5 nmol Zn-mesoporphyrin formed/ 10^6 cells/h at 37°C with IVS3-48T/T. * $P < 0.01$, C:T versus T:T; ** $P < 0.005$, C:C versus T:T

HPLC with 5C18-5AR column (4.6×150 mm) (Nacalai Tesque, Kyoto, Japan). As shown in Fig. 1, the highest activity was observed in the genotype with IVS3-48T/T, a moderate level was shown with IVS3-48C/T, and the lowest level was with IVS3-48C/C. The FECH activity with IVS3-48C/C was only 38% of that with IVS3-48T/T. Then, we compared the FECH activities in EPP patients with those in healthy controls with IVS3-48C/C, C/T and T/T. As shown in Fig. 2, the activities in EPP patients relative to those of the controls were divided into three groups, which corresponded to 15, 35 and 64% of the controls, and these were dependent on the three genotypes. Various investigators have found that the FECH activities in EPP patients vary widely (8-45%), compared with those in controls [1, 9]. Some researchers reported that EPP seemed to exhibit

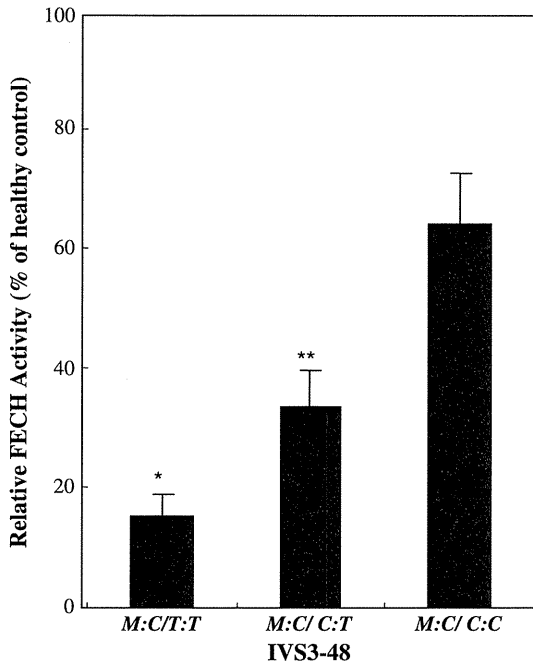


Fig. 2 The FECH activity in EPP patients relative to that of healthy controls with IVS3-48C/T transition. The FECH activity in peripheral blood lymphocytes of patients with EPP (*M:C*) was measured by comparison with that of controls with IVS3-48T/T (*T:T*) ($n = 4$), IVS3-48C/T (*C:T*) ($n = 6$) and IVS3-48C/C (*C:C*) ($n = 5$) of the gene. * $P < 0.01$, *M:C/T:T* versus *M:C/C:C*; ** $P < 0.01$, *M:C/C:T* versus *M:C/C:C*

autosomal recessive inheritance owing to the low enzyme activity [10]. We now demonstrate that this variation is derived from the three different genotypes of the *FECH* gene. Thus, heterozygotes with the low expression allele (IVS3-48C) in combination with a null allele would produce a small amount of FECH when compared with the normal group. Similarly, a low expression allele combined with a missense allele could explain the weak FECH activity observed in patients with EPP. Conversely, the FECH activities in healthy controls varied, the level of the relative FECH activities in EPP patients differed, depending on the different activities from the IVS3-48 genotypes of the *FECH* gene among controls. To estimate the frequency of IVS3-48C/T transition of the *FECH* gene in the Japanese population, analysis by single-strand conformation polymorphism (SSCP) using GeneGel Excel 12, 5/24 kit (GE Bioscience, Buckinghamshire, UK) was carried out with the genomic DNA of healthy volunteers. Of the 148 Japanese examined, the genotype with IVS3-48C/C was found in 32 (22%), IVS3-48C/T was in 68 (46%) and IVS3-48T/T was in 48

(32%). Thus, over half of the subjects have IVS3-48C. This value is similar to those reported for Asian people [2, 7]. Given that 10% of Caucasians have IVS3-48C, Asian people including Japanese face a higher risk of EPP. Although the reduced FECH activity is an important factor to diagnose EPP, it is difficult to evaluate EPP by FECH activity because of the high frequency of healthy controls with IVS3-48C in Asian populations.

Acknowledgments This work was supported in part by a Grant from the Ministry of Health, Labor and Welfare of Japan.

References

1. Taketani S, Fujita H. The ferrochelatase gene structure and molecular defects associated with erythropoietic protoporphyria. *J Bioenerg Biomembr.* 1995;27(2):231–8.
2. Gouya L, Martin-Schmitt C, Robreau AM, Austerlitz F, Da Silva V, Brun P, Simonin S, Lyoumi S, Grandchamp B, Beaumont C, Puy H, Deybach JC. Contribution of a common single-nucleotide polymorphism to the genetic predisposition for erythropoietic protoporphyria. *Am J Hum Genet.* 2006;78(1):2–14.
3. Taketani S, Inazawa J, Nakahashi Y, Abe T, Tokunaga R. Structure of the human ferrochelatase gene. Exon/intron gene organization and location of the gene to chromosome 18. *Eur J Biochem.* 1992;205(1):217–22.
4. Gouya L, Puy H, Lamoril J, Da Silva V, Grandchamp B, Nordmann Y, Deybach JC. Inheritance in erythropoietic protoporphyria: a common wild-type ferrochelatase allelic variant with low expression accounts for clinical manifestation. *Blood.* 1999;93(6):2105–10.
5. Gouya L, Puy H, Robreau AM, Bourgeois M, Lamoril J, Da Silva V, Grandchamp B, Deybach JC. The penetrance of dominant erythropoietic protoporphyria is modulated by expression of wildtype FECH. *Nat Genet.* 2002;30(1):27–8.
6. Schoenfeld N, Mamet R, Minder EI, Schneider-Yin X. A “null allele” mutation is responsible for erythropoietic protoporphyria in an Israeli patient who underwent liver transplantation: relationships among biochemical, clinical, and genetic parameters. *Blood Cells Mol Dis.* 2003;30(3):298–301.
7. Nakano H, Nakano A, Toyomaki Y, Ohashi S, Harada K, Moritsugu R, Takeda H, Kawada A, Mitsunashi Y, Hanada K. Novel ferrochelatase mutations in Japanese patients with erythropoietic protoporphyria: high frequency of the splice site modulator IVS3-48C polymorphism in the Japanese population. *J Invest Dermatol.* 2006;126(12):2717–9.
8. Taketani S. Measurement of ferrochelatase activity. In: Maines MD, Costa LC, Reed DJ, Sassa S, Sipes JG, editors. 1999 Current protocol in toxicology, vol 1, Suppl 2. New York: Wiley, unit 8.7.1–8.7.8.
9. Elder GH, Gouya L, Whatley SD, Puy H, Badminton MN, Deybach JC. The molecular genetics of erythropoietic protoporphyria. *Cell Mol Biol (Noisy-le-grand).* 2009;5(2):118–26.
10. Sarkany RP, Alexander GJ, Cox TM. Recessive inheritance of erythropoietic protoporphyria with liver failure. *Lancet.* 1994;343(8910):1394–6.

Porcine Ferrochelatase: The Relationship between Iron-Removal Reaction and the Conversion of Heme to Zn-Protoporphyrin

Tuan Thanh CHAU,¹ Mutsumi ISHIGAKI,¹ Takao KATAOKA,¹ and Shigeru TAKETANI^{1,2,†}

¹Department of Biotechnology, Kyoto Institute of Technology, Kyoto 606-8585, Japan

²Insect Biomedical Center, Kyoto Institute of Technology, Kyoto 606-8585, Japan

Received February 2, 2010; Accepted April 19, 2010; Online Publication, July 7, 2010

[doi:10.1271/bbb.100078]

At the terminal step of heme biosynthesis, ferrochelatase (FECH) catalyzes the insertion of Fe²⁺ into protoporphyrin to form heme. It is located on the inner membrane of the mitochondria of animals. The enzyme inserts divalent metal ions, including Fe²⁺, Co²⁺, and Zn²⁺, into porphyrins *in vitro*. We have reported that it can remove Fe²⁺ from heme. To characterize the iron-removal reverse activity of FECH, we examined its properties in porcine liver and muscle mitochondria, and isolated porcine FECH cDNA. The amino acid sequence of porcine FECH showed high homology with bovine (91%), human (85%), mouse (87%), and rat (76%) equivalents. It was expressed in *Escherichia coli*, and purified, and the kinetic properties of the zinc-chelating and iron-removal activities were examined. Both activities peaked at 45 °C, but different optimal pH values, of 7.5–8.0 for zinc-ion insertion and 5.5–6.0 for the reverse reaction were found. The K_m values for mesoporphyrin IX and Zn²⁺ were 6.6 and 1.1 μM, respectively, and the K_m for heme was 5.7 μM. The k_{cat} value of the forward reaction was about 11-fold higher than that of the reverse reaction, indicating that the enzyme preferably catalyzes the forward reaction rather than the iron-removal reaction. Reverse activity was stimulated by fatty acids and phospholipids, similarly to the case of the forward reaction, indicating that lipids play a role in regulating both enzyme activities.

Key words: ferrochelatase; iron-removal reaction; Zn-protoporphyrin; porcine muscle mitochondria; cDNA cloning

At the terminal step of the heme-biosynthesis pathway, ferrochelatase (FECH) (EC 4.99.1.1), located on the inner membrane of the mitochondria, catalyzes the insertion of ferrous ions into protoporphyrin IX to form protoheme.¹ FECH protein has a molecular mass of 40–42 kDa on SDS–PAGE analysis. Mammalian FECH is active as an homodimer, as analyzed by radiation inactivation and X-ray crystallography,^{2,3} and contains an iron-sulfur cluster as a functional group.^{3,4} Some lipids promote its enzyme activity,^{1,5} while this activity is inhibited by heavy metal ions, such as lead and mercury.¹ Ferrous ions are the target of the enzyme

in vivo, while other divalent metal ions, including zinc, cobalt, and tin, are also utilized to form other metalloporphyrins *in vitro*.^{1,6}

Both the cDNA and the gene for FECH have been isolated and sequenced from micro-organisms, plants, and animals, including humans, the cow, the mouse, and the rat.² The mammalian enzymes from humans, the bovine, the mouse and the rat have been expressed in the active form in *E. coli*. The kinetic properties of the enzyme were examined.^{1,2}

Although iron is an essential element for living cells, an excess of intracellular ferric ions can be toxic.⁷ Uncommitted heme in the cells is also very dangerous for the maintenance of living systems.^{8,9} Therefore, reutilization of iron, including degradation of the heme, catalyzed by heme oxygenase, is essential for the homeostasis of iron in cells. Recently, we reported that the removal of ferrous ions from heme occurred *in vivo*, and that FECH removed iron from heme *in vitro*,¹⁰ but the role of the reaction in removing iron *in vivo* is not clear.

The red pigment of cured ham is usually due to nitrosomyoglobin, a product of the thermal treatment of meat with nitrite. Nitrosamines can be generated in that process during storage or shelving period.^{11,12} Therefore, nitrite-free ham is a preferred alternative. Dry-cured ham (Parma ham), which is nitrite-free, is made from porcine muscle with only sea salt at a suitable temperature for long periods.¹³ The main component of the red pigment of the ham has been found to be Zn-protoporphyrin,^{10,14} a pigment stable under air exposure and heating.¹⁵ Although the mechanism involved in the formation of Zn-protoporphyrin during the production of dry ham is unclear, formation in the muscle may be related to mitochondria and enzyme catalysis.¹⁶ Very recently, we found that FECH is involved mainly in the formation of Zn-protoporphyrin *via* iron-removal reverse reaction,¹⁰ but little attention has been paid to the characteristics and kinetic properties of the reverse reaction of FECH.

Here, we characterized FECH in porcine liver and muscle mitochondria. Then we isolated the FECH cDNA, the actively expressed enzyme in *E. coli*, and purified it. The catalytic properties of the forward and reverse reactions were compared.

The nucleotide sequence will appear in the Genbank/DDBJ Nucleotide Sequence Database under accession no. AB530166.

† To whom correspondence should be addressed. Fax: +81-75-724-7789; E-mail: taketani@kit.ac.jp

Abbreviations: FECH, ferrochelatase; SDS–PAGE, sodium dodecylsulfate-polyacrylamide gel electrophoresis; MDH, malate dehydrogenase

Materials and Methods

Materials. Restriction endonucleases and DNA-modifying enzymes were obtained from Takara (Tokyo) and Toyobo (Tokyo). Mesoporphyrin IX, protoporphyrin IX, and Zn-protoporphyrin were from Frontier Scientific (Logan, UT). Hemin-imidazole was prepared as previously described.¹⁰ Pig kidney LLC-PK1 cells were obtained from the Japan Cell Bank (Saitama, Japan). Porcine livers and muscles were generously donated by Itoh Ham Inc. (Moriya, Japan). The antibodies for ferrochelatase used were as described previously¹⁷ and the antibodies for malate dehydrogenase (MDH) were obtained from Calzyme Laboratories (San Luis, CA). All other chemicals used were of analytical grade.

Isolation of mitochondria. Pig muscle and liver were suspended in 10 mM Tris-HCl (pH 7.5), 0.25 M sucrose (6.0 ml/g) and homogenized at 4°C. The homogenates were centrifuged at 600 × g for 10 min at 4°C, and then the supernatants were centrifuged at 12,000 × g for 10 min at 4°C. After they were washed twice, the pellets (mitochondrial fraction) were dissolved with the above solution and stored at -20°C. The protein concentration was measured by the method of Lowry *et al.*¹⁸ or that of Bradford,¹⁹ using BSA as standard.

DNA cloning. Total RNA was isolated from LLC-PK1 cells using RNAsol Super (Nacalai Tesque, Kyoto, Japan), and poly(A)⁺-rich RNA was obtained with oligo(dT) cellulose (GE Healthcare, Buckinghamshire, UK). Single-strand cDNA was synthesized using an oligo(dT) primer (GE Healthcare). For isolation of porcine FECH cDNA, several primers for PCR were designed on the basis of the cDNA of human, mouse, and bovine FECH. The primers finally used for DNA amplification were as follows: forward (PoF1: 5'-AAGAATTCAATGCTTTCAGTCGGCAC-3'), and reverse (PoR: 5'-AAAAGCTTCACAGCTGGCTGGT-3'). After PCR was completed, the product was separated on a 1.1% agarose gel, digested with *Eco*RI and *Hind*III, and ligated into *Eco*RI/*Hind*III-digested pBluescript II KS⁺ vector (Stratagene, La Jolla, CA). The inserted fragment of the plasmid was confirmed by determining the nucleotide sequence.

Expression of porcine FECH. To express porcine FECH in bacteria, the cDNA was amplified with a second forward primer (PoF2: 5'-AAGAATTCAAGCCCCAACTTCAAGT-3') and the reverse primer PoR described above. The resulting DNA fragment was ligated into *Eco*RI/*Hind*III-digested pET carrying His-tagged expression vector (Merk, Darmstadt, Germany), and the plasmid obtained was transferred to *E. coli*, BL21. The bacteria were grown in LB medium for 16 h, and then the culture medium was diluted by 10-fold in fresh LB medium. The enzyme was expressed with 0.3 mM isopropyl- β -D-thiogalactopyranoside at 30°C for 2 h.

Purification of recombinant ferrochelatase. The cells were harvested by centrifugation and suspended in 20 mM Tris-HCl (pH 8.0), 10% glycerol, 1 mM DTT, 0.1% Tween 20, 20 mM imidazole, and 0.3 M NaCl. They were disrupted by sonication and centrifuged at 5,000 × g at 4°C for 10 min. The supernatants were shaken with Ni²⁺-NTA beads (Qiagen, Valencia, CA), and washed 3 times with the above solution. The enzyme was eluted with 20 mM Tris-HCl (pH 8.0), 10% glycerol, 0.1% Tween 20, 0.25 M imidazole, and 0.3 M NaCl.

Immunoblotting. The proteins were analyzed by SDS-PAGE, and stained with Coomassie Brilliant Blue or electroblotted onto a polyvinylidene difluoride membrane. Immunoblotting was carried out using anti-ferrochelatase as primary antibody.¹⁶

Enzyme assay. FECH activity was determined by measuring the insertion of zinc into mesoporphyrin, as described previously.²⁰ For examination of the reverse activity of FECH, a reaction mixture containing 10 μ M hemin-imidazole, 2 mM ascorbic acid and 10 mM potassium phosphate buffer (pH 5.5) in a final volume of 1.0 ml in a Thunberg vacuum tube was used. The dissolved gas was removed *in vacuo*. The reaction was carried out at 45°C for 1 h. To measure the conversion of heme to zinc-protoporphyrin, 20 μ M zinc ions was added to the reaction mixture. After incubation, the protoporphyrin or zinc-protoporphyrin formed was measured fluorophotometrically.¹⁰

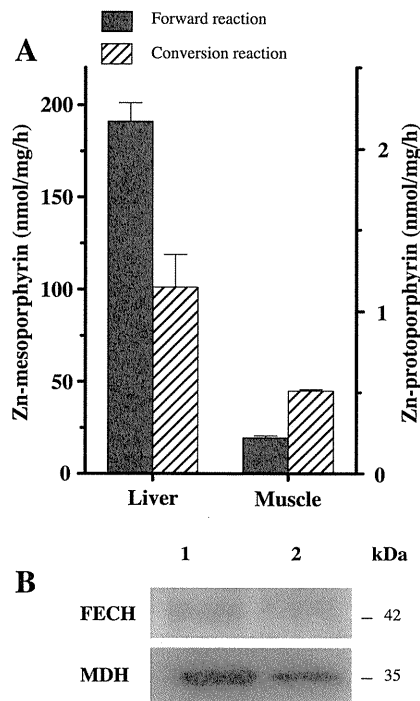


Fig. 1. Characterization of Porcine FECH in the Muscle and Liver, and the Activity of Porcine Liver and Muscle FECH.

A. For the forward reaction, liver and muscle mitochondria were incubated with 20 mM Tris-HCl, pH 8.0, 0.1% Tween 20, 15 μ M mesoporphyrin IX, and 40 μ M zinc acetate in a final volume of 200 μ l at 37°C for 60 min. The formation of Zn-mesoporphyrin was measured. Data are expressed as mean \pm SD of triplicate experiments. For the conversion of heme to Zn-protoporphyrin, a reaction mixture containing liver or muscle mitochondria (0.2–1.0 mg, protein), 10 mM potassium phosphate buffer, pH 5.5, 10 μ M hemin-imidazole, 50 μ M zinc acetate, and 200 μ M NADH was used, in a final volume of 1.0 ml. The reaction was carried out at 45°C for 60 min. The formation of Zn-mesoporphyrin or Zn-protoporphyrin was measured. Data are expressed as mean \pm SD of triplicate experiments. **B.** Immunoblot analysis. Immunoblotting was performed with liver (lane 1) and muscle (lane 2) mitochondria, using anti-FECH and anti-MDH as the primary antibodies. Liver and muscle mitochondria (5 μ g of protein) loaded into slots were used.

Results

Characterization of FECH in porcine liver and muscle

To characterize muscle FECH, mitochondria were isolated from porcine liver and muscle by centrifugation and FECH activity was examined. The formation of Zn-mesoporphyrin in the muscle mitochondria was much lower than in the liver mitochondria (Fig. 1A). We also examined the reverse activity of FECH by measuring the conversion of heme to Zn-protoporphyrin. The conversion activity in the muscle mitochondria was about 40% of that in the liver mitochondria (Fig. 1A). Then the proteins in the mitochondria were analyzed by SDS-PAGE and transferred onto a membrane, and immunoblotting was performed using antibodies for bovine FECH and for the mitochondrial matrix protein, MDH (Fig. 1B). The results indicated that FECH was expressed in both tissues, and the amount of FECH in the muscle was low as compared with that of the hepatic enzyme.

Cloning of porcine FECH cDNA

To isolate porcine FECH cDNA, mRNA was isolated from kidney LLC-PK1 cells, and PCR using specific

Porcine	1	MLSVGTNMAAALRS	GA	VLLRDL	LVYGGSRACQPWR	RCOSGMA	AAAA--EAVQ	HARSPK	PQV	58
Bovine	1	-----MAAALRS	GA	VLLRDL	LVYGGSRACQPWR	RCOSGAA	TAAAA	TETAQ	RA	53
Human	1	MRLSGANMAAALRA	AGVLLR	DLPLASS	WRVCPWR	RKSGAAAA	AVTTE	TAQHA	QGA	60
Mouse	1	MLSASANMAAALRA	AGVLLR	DLPLVH	SSRACQPWR	RCOSGAA	VAAAT	TEKV	-HAK	59
Rat	1	MAVLGC---	ACRLVQ	-LVR	CGSPVGLCLSS	SL--RRO	ST-ATA	A	AFNTT	47
Porcine	59	QTGNR	RKPKTG	ILMLN	MGGPET	TVGEV	QDFL	RRL	FLD	118
Bovine	54	QPGNR	RKPKTG	ILMLN	MGGPET	VVEEV	QDFL	QRL	FLD	113
Human	61	QPQRK	RKPKTG	ILMLN	MGGPET	LGDVH	DFLL	RRL	FLD	120
Mouse	60	QPERR	RKPKTG	ILMLN	MGGPET	TVGEV	QDFL	QRL	FLD	119
Rat	48	K-ESR	RKPKTG	ILMLN	MGGPE	KLEDV	HDFLL	RRL	FMD	106
Porcine	119	EQYRR	IGGGSP	IKMWT	SKQEG	GMVKLL	DELSP	H	TAPHK	178
Bovine	114	EQYRR	IGGGSP	IKMWT	SKQEG	GMVKLL	DELSP	H	TAPHK	173
Human	121	EQYRR	IGGGSP	IKMWT	SKQEG	GMVKLL	DELSP	H	TAPHK	180
Mouse	120	EQYRR	IGGGSP	IKMWT	SKQEG	GMVKLL	DELSP	H	TAPHK	179
Rat	107	EQYSK	IGGGSP	IKAWT	TMQEG	GMVKLL	DEMCP	D	TAPHK	166
Porcine	179	GLERA	IAFTQY	PQYSC	ATTG	SSLN	AIYRY	YNEV	GKPT	238
Bovine	174	GLERA	IAFTQY	PQYSC	TTG	SSLN	AIYRY	YNEV	GKPT	233
Human	181	GLERA	IAFTQY	PQYSC	TTG	SSLN	AIYRY	YNQV	GRKPT	240
Mouse	180	GLERA	IAFTQY	PQYSC	TTG	SSLN	AIYRY	YNEV	GKPT	239
Rat	167	GVERA	IAFTQY	PQYSC	TTG	SSLN	AIYRY	YSNR	ADRP	226
Porcine	239	ILKEL	DHFPE	EKRRE	VVILF	SAHSLP	MSV	VNR	GD	298
Bovine	234	ILKEL	DHFPE	EKRRE	VVILF	SAHSLP	MSV	VNR	GD	293
Human	241	ILKEL	DHFPE	EKRRE	VVILF	SAHSLP	MSV	VNR	GD	300
Mouse	240	ILKEL	NHFPE	EKRRE	VVILF	SAHSLP	MSV	VNR	GD	299
Rat	227	VRNEL	DKFPE	EKRRE	VVILF	SAHSLP	PLSV	VNR	GD	286
Porcine	299	WQSKV	GPM	WLG	PQ	TDEA	IKGL	C	ER	358
Bovine	294	WQSKV	GPM	WLG	PQ	TDEA	IKGL	C	ER	353
Human	301	WQSKV	GPM	WLG	PQ	TDES	IKGL	C	ER	360
Mouse	300	WQSKV	GPM	WLG	PQ	TDEA	IKGL	C	ER	359
Rat	287	WQSKV	GPM	WLG	PQ	TDEA	IKGL	C	ER	346
Porcine	359	GAENI	RAESL	NGN	PLFS	KALAD	LVH	SHI	Q	418
Bovine	354	GAENI	RAESL	NGN	PLFS	KALAD	LVH	SHL	Q	413
Human	361	GVENI	RAESL	NGN	PLFS	KALAD	LVH	SHI	Q	420
Mouse	360	GAENI	RAESL	NGN	PLFS	KALAD	LVH	SHI	Q	419
Rat	347	GVENI	RAESL	NGN	PLFF	RALAD	LVQ	SHL	Q	406
Porcine	419	QQT								421
Bovine	414	QQT								416
Human	421	QQT								423
Mouse	420	QQT								422
Rat	407	QQT								409

Fig. 2. Amino Acid Sequence Alignment of Porcine, Bovine, Human, Mouse, and Rat FECH.

Amino acids identical among the five species are boxed. Asterisks show the conserved cysteine residues for the iron-sulfur cluster.

primers was carried out. A DNA fragment of about 1.2 kb was obtained and ligated into pBluescript vector, and the plasmids obtained were sequenced. The nucleotide sequence showed a high homology to the bovine, human, mouse and rat equivalents. Figure 2 shows an alignment of the porcine, bovine, human, mouse, and rat amino acid sequences. The overall homologies of the porcine enzyme were 91% with the bovine enzyme, 85% with the human, 86% with the mouse, and 76% with the rat. There were many highly conserved regions and four cysteine residues at the C-terminus of the iron-sulfur cluster among the mammalian enzymes.

Expression and purification of FECH in *E. coli*

We constructed an expression plasmid, pET-pFECH, and was transferred to *E. coli* strain BL21. Protein expression was induced by incubation with 0.3 mM IPTG at 30 °C for 2 h. When the enzyme activity was measured using cell extracts of untransformed and transformed bacteria, the rates of both the forward and the reverse reaction in the transformed cells were high as compared to those in the control, indicating that the enzyme was active (Fig. 3A). The activity of the conversion of heme to Zn-protoporphyrin in extracts of FECH-expressing cells was similar to the reverse activity. His-tagged FECH was then purified with Ni-NTA agarose beads. The purified His-tagged FECH was

analyzed by 10% SDS-PAGE and stained with Coomassie Brilliant Blue (Fig. 3B). A specific band with a molecular mass of 42 kDa was found, and the specific enzyme activity increased by about 20-fold after purification. Immunoblot analysis revealed that the protein reacted with anti-FECH antibody (Fig. 3C).

Kinetic properties of purified FECH

When enzyme activity was examined with the purified FECH, the conversion of heme to Zn-protoporphyrin as well as iron-removal reaction occurred in a similar fashion.

When the temperature of the reaction was changed, the forward and reverse activities peaked at 45 °C (Fig. 4A). Figure 4B shows the pH profile of the forward and iron-removal reverse reactions. The zinc-insertion reaction showed high activity at pH 7.5–8.0, while the reverse reaction showed high activity at pH 5.5–6.0.

The K_m of the forward reaction for mesoporphyrin IX and zinc were 6.6 and 1.1 μM , respectively (Table 1). The k_{cat} value of the enzyme for the two subjects was estimated to be 400 min^{-1} . The ratio k_{cat}/K_m of mesoporphyrin IX is approximately 6-fold higher than that of zinc acetate. This means that the reaction velocity depends on mainly the mesoporphyrin IX concentration in the reaction mixture. For the reverse reaction, the values of K_m and k_{cat} of hemin were estimated to be

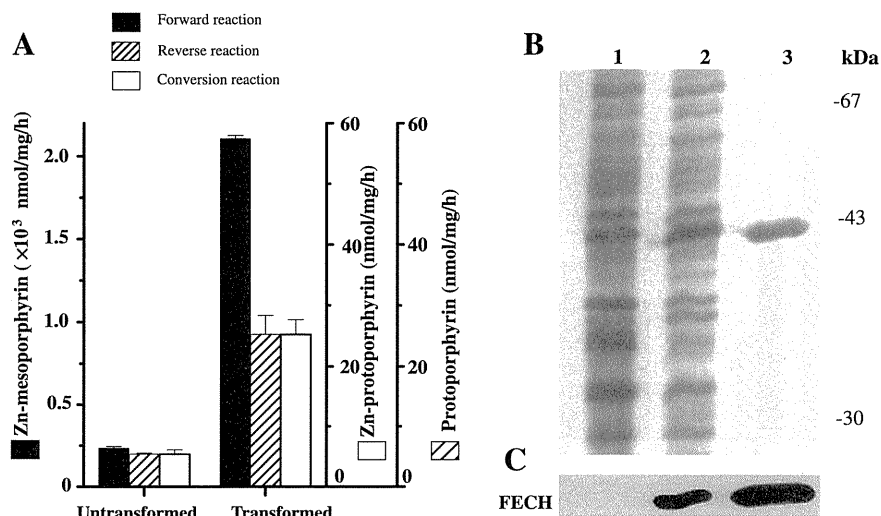


Fig. 3. The Molecular Properties of Recombinant Porcine FECH Expressed in *E. coli*.

A, FECH activity. Supernatants obtained by centrifugation from control (lane 1) and FECH-expressing *E. coli* (lane 2) were used to measure the forward, reverse, and conversion reactions, which were performed similarly to the description in the legend to Fig. 1. Data are expressed as the mean \pm SD of triplicated experiments. **B**, SDS-PAGE analysis. The proteins in the supernatants as above (lanes 1 and 2) and FECH purified using Ni-NTA beads (lane 3) were analyzed by SDS-PAGE and stained with Coomassie Brilliant Blue. **C**, Immunoblot analysis. Immunoblotting was performed using anti-FECH as the primary antibody.

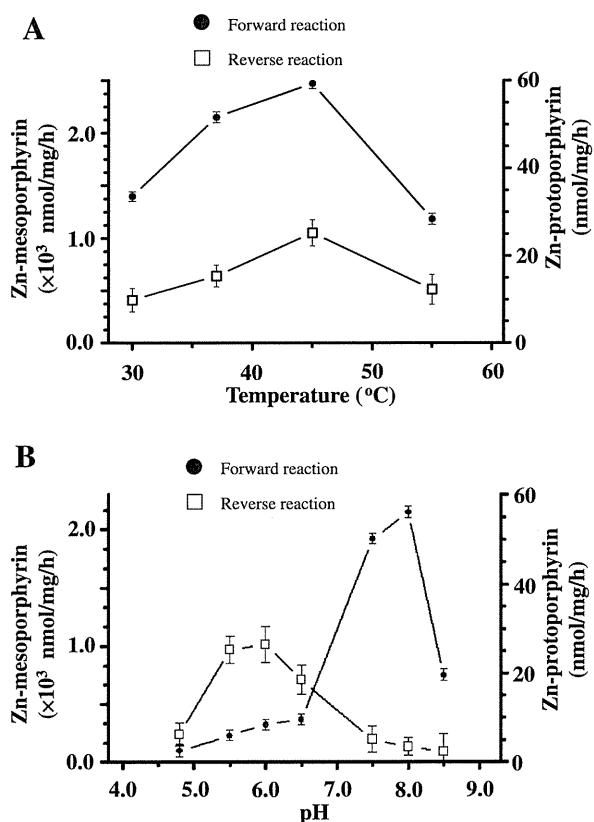


Fig. 4. Characterization of Forward and Reverse Reactions of Recombinant FECH.

A, effects of temperature (A) and pH (B). FECH activity was measured with mesoporphyrin IX and zinc acetate for the forward reaction. The reverse reaction was performed using hemin-imidazole as substrate. Data are expressed as the mean \pm SD of duplicate experiments.

5.7 μM and 31.4 min^{-1} respectively, suggesting that FECH proceeded readily in the forward reaction.

Previous studies^{1,5,21} have found that FECH activity increases owing to various lipids including fatty acids and phospholipids. To determine the effects of fatty

Table 1. Kinetics of FECH

Parameter	Forward reaction*		Reverse reaction*
	Mesoporphyrin IX	Zinc	Hemin
K_m (μM)	6.6 \pm 0.2	1.1 \pm 0.1	5.7 \pm 0.2
k_{cat} (min^{-1})	400.0 \pm 38.0		31.4 \pm 2.4
k_{cat}/K_m ($\mu\text{M}^{-1} \cdot \text{min}^{-1}$)	60.7 \pm 6.0	351.2 \pm 45.7	5.5 \pm 0.5

*The assay conditions used were as described in "Materials and Methods." Data are expressed as the mean \pm SD of 2–4 experiments.

acids on iron-removal reverse activity, we added sodium palmitate to the reaction mixture. Upon increasing the concentration of sodium palmitate to 100 $\mu\text{g}/\text{ml}$, the forward and reverse activities increased concentration-dependently, and the rates of the forward and reverse reactions increased 2.5-fold and 2.0-fold in the presence of 100 $\mu\text{g}/\text{ml}$ sodium palmitate, respectively (Fig. 5A). Other fatty acids such as stearic acid and oleic acid showed activities similar to those of palmitic acid. At 100 $\mu\text{g}/\text{ml}$, phosphatidylcholine, the rate of forward activity increased while that of the reverse reaction decreased. Lysophosphatidylcholine slightly activated forward activity, but inhibited reverse activity. Sphingomyelin and lysophosphatidic acid markedly inhibited reverse but not forward activity.

Finally, we examined the effects of heavy metal ions on iron-removal reverse activity. As shown in Fig. 5B, the reaction was markedly inhibited by ferric and cubic ions, but ferrous, cobaltic, and tin ions had no effect.

Discussion

We characterized porcine FECH located in the liver and muscle mitochondria. The amount and activity of FECH in the muscle mitochondria were low compared with those in the hepatic mitochondria. In addition to